

# EMI Noise Prediction for Electronic Ballasts

Florian Giezendanner\*, Jürgen Biela\*, Johann Walter Kolar\*, Stefan Zudrell-Koch\*\*

\*Power Electronic Systems Laboratory, ETH Zurich, Zurich, Switzerland

\*\*TridonicAtco Lighting, Faerbergasse 15, 6850 Dornbirn, Austria

**Abstract**—The design of EMI-filters for converter systems is usually based on measurements with a prototype in the final stages of the design process. Predicting the conducted electromagnetic (EM) noise spectrum of a converter by simulation in an early stage has the potential to save time/cost and to investigate different noise reduction methods, which could e.g. influence the layout or the design of the control IC.

Therefore, the main sources of conducted differential mode (DM) and common mode (CM) noise of electronic ballasts are identified in this paper. For each source, the noise spectrum is calculated and a noise propagation model is presented. There, also the influence of the LISN and the test receiver is included.

Based on the presented models noise spectrums are calculated and validated by measurements.

## I. INTRODUCTION

In **Fig. 1** a typical circuit of a two-stage electronic ballast is shown. The basic functions of the inverter stage are: 1) generation of the filament current and lamp voltage to ensure the ignition of the lamp, 2) operation of the lamp with a sinusoidal current typically at a frequency of 40 – 50 kHz because of EMI reasons. The inverter stage is often realized using a load-resonant half-bridge topology [1]. An active power factor correction (PFC) stage is required in order to meet the regulations for the input current harmonics and to realize a near-unity power factor. The PFC stage is realized with a boost converter operating at the border between discontinuous and continuous current conduction (so called boundary conduction mode (BCD) or critical conduction mode), which is the standard for power levels required by ballasts for fluorescent lamps.

The high-frequency operation of the PFC stage and the inverter causes conducted noise on the input line and radiated electromagnetic noise in the environment of the ballast. In order to prevent interference with other systems, custom designed EMI filters are

required to meet the limits for conducted and radiated EM noise, which are regulated in international standards. In the European Union, the relevant standards for lighting systems are EN55015 for conducted and radiated EMI in the range 9 kHz - 30 MHz and EN55015 or EN55022 for radiated noise in the range 30 MHz - 1 GHz.

The conventional way to design an EMC input filter is to build a prototype of the system with an initial filter derived by approximate calculations or experience. The final filter design is found by iterative EMC measurements and modification of the filter until the standards are met with minimal cost of the filter components.

An alternative approach for designing an input filter is to simulate the conducted EM noise of the converter [2-5]. Using a simulation has the potential to avoid expensive and time-consuming redesigns of the hardware prototypes. Furthermore, the influence of the modulation, topological modifications, layout, etc. can be investigated before building hardware. Therefore, a simulation model for predicting the conducted EM noise spectrum of electronic ballasts for fluorescent lamps is presented and validated in this paper, where the focus is put on the PFC input stage in a first step. Further results including also the inverter stage will be presented in a future paper.

The main challenge for EMI simulations is that the EM noise generation in a converter system is highly dependent on circuit and semiconductor parasitics, which are difficult to model and lead to very complex simulations. Therefore, the most important part of this work is to identify the main sources of differential mode (DM) and common mode (CM) noise and the corresponding propagation paths in electrical ballasts and to derive robust and computationally efficient models for the EMI behavior of the ballast.

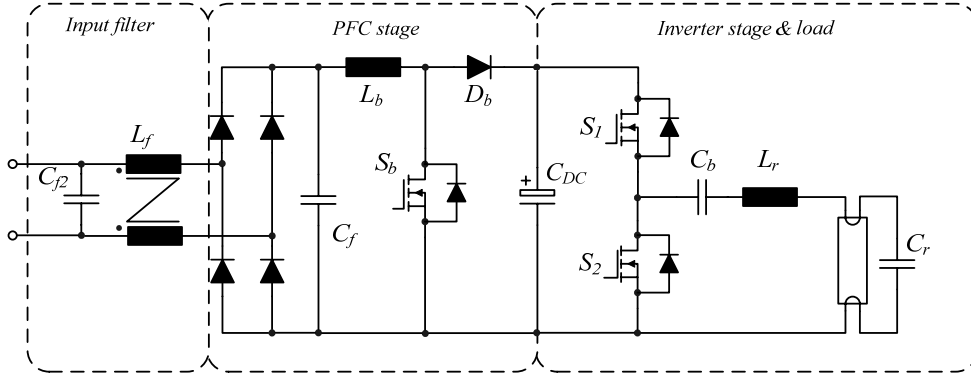


Fig. 1 Typical circuit of a two-stage electronic ballast.

The simulation approach presented in this paper is based on the calculation of the waveforms of each noise source in the time-domain followed by a fast Fourier transform to calculate the spectrum of the noise source. Then, a noise propagation transfer function is identified for each source in order to calculate the spectrum at the input of the EMC test receiver from the noise source spectrum. Therefore, in **Section II** the modeling of the test receiver including the LISN, the input cable and the EMC test receiver is described. In **Section III**, the main noise sources for DM and CM noise are identified and the noise propagation models are presented. **Section IV** describes the implementation of the model in a *Java* program. Finally, the comparison of the simulation results with measurements is presented in **Section V**.

## II. TEST SETUP MODELING

The setup for conducted EMI measurements consists of a line impedance stabilizing network (LISN), the input cable and an EMC test receiver (cf. **Fig. 2**). The LISN presents a defined impedance between the mains and the device under test (DUT) in order to guarantee the reproducibility of the measurements. Additionally, it provides an interface between the DUT and the test receiver. The EMC test receiver is a specialized spectrum analyzer implementing the measurement procedures specified in the EMC standards (e.g. CISPR-16).

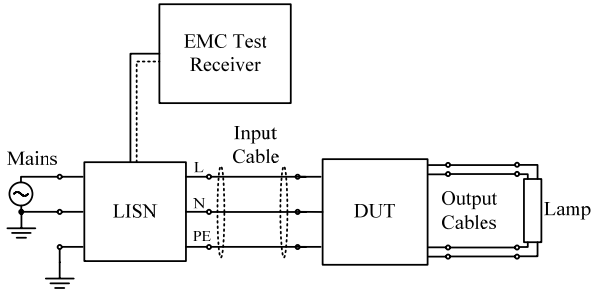


Fig. 2 Conducted noise emission measurement setup

### A. Model of the LISN

The circuit diagram of a single-phase LISN according to CISPR-16 is shown in **Fig. 3 a)**. For frequencies above 9 kHz, the influence of the filter stage comprising  $L_2$ ,  $C_2$  and  $R_2$  on the impedance of the LISN can be neglected. Therefore, the simplified model shown in **Fig. 3 b)** is used for in the presented simulations. The voltage  $V_{rec}$  is the noise voltage at the input of the test receiver, which has an input resistance  $R_{in}$  of 50  $\Omega$ .

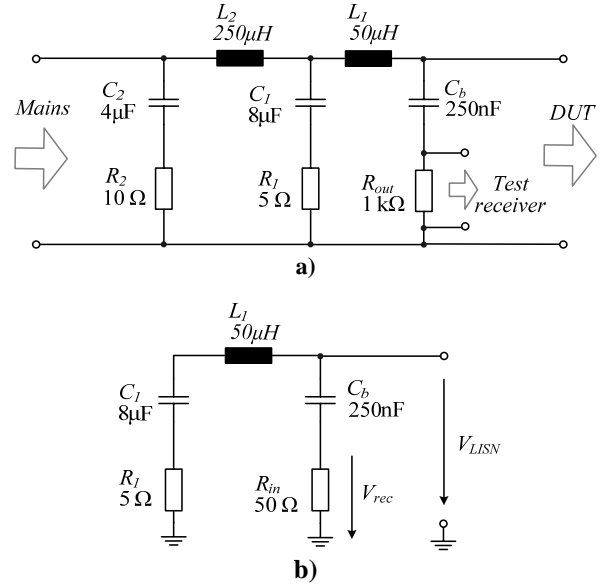


Fig. 3 a) Schematic of a LISN according to CISPR-16. b) Simplified model applied in the simulation.

### B. Model of the test receiver

**Fig. 4** shows a simplified block diagram of a test receiver based on the super-heterodyne principle. The input voltage is buffered and attenuated in the first stage and applied to a mixer which multiplies the attenuated signal with the output of a tuneable local oscillator. The output of the mixer is the input signal shifted by the output frequency of the local oscillator, allowing to select the part of the input spectrum which is mapped to the center frequency of the intermediate frequency (IF) filter by tuning the frequency of the oscillator.

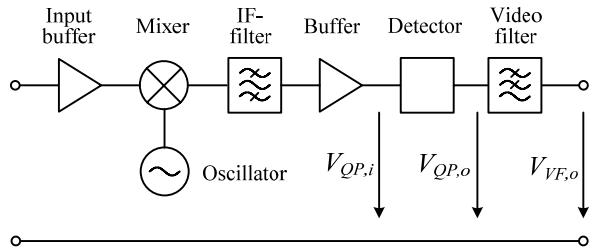


Fig. 4 Simplified block diagram of an EMC test receiver.

In CISPR-16, different IF-filters are defined depending on the frequency range of interest. In Band A (9 kHz – 150 kHz) the 6dB bandwidth is 200 Hz, in Band B (150 kHz – 30 MHz) 9 kHz (cf. **Table 1**).

	Band A 9 kHz - 150 kHz	Band B 150 kHz - 30 MHz
IF-filter bandwidth	200 Hz	9 kHz
QP charging time constant	45 ms	1 ms
QP discharging time constants	500 ms	160 ms
Mechanical time constant	160 ms	160 ms

**Table 1** Filter bandwidth and time constants according to CISPR-16.

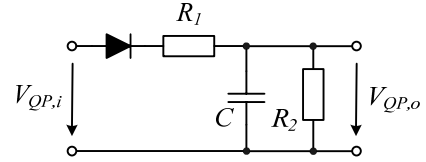
Several detector types are used for EMC measurements: quasi-peak (QP), peak, average and rms. The final stage of the test receiver is a mechanical time constant defined in the standard for moving coil meters, which is equivalent to a critically damped second-order low-pass filter.

In the simulation model, the band-pass filtering is done in the frequency domain, where the operation of the mixer and IF-filter is equivalent to the multiplication of the input spectrum with the previously calculated frequency response of the filter shifted to the frequency under consideration.

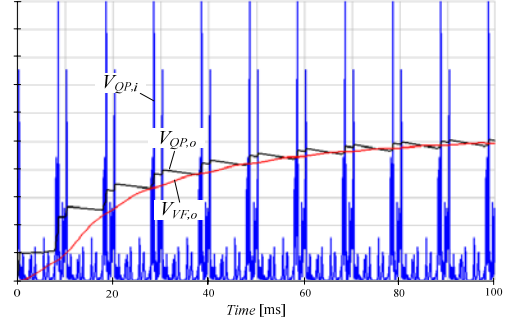
For an accurate simulation of the detectors, the time-domain voltage waveform at the input of the detector has to be calculated for one mains half-period. For a certain frequency  $f$  under consideration, this is done by multiplication of the input spectrum with the response of the IF-filter shifted to  $f$  and a subsequent inverse fast Fourier transform (IFFT). The output of the peak detector is the maximum of the resulting voltage waveform.

**Fig. 5 a)** shows the circuit of a quasi-peak detector. The resistors  $R_1$  and  $R_2$  set the time-constants for charging and discharging the capacitor  $C$  as defined in CISPR-16 (see **Table 1**). Due to the discharge, the output of the quasi-peak detector depends not only on the amplitude envelope of the incoming signal, but also on the pulse repetition rate.

The simulation model of the quasi-peak detector is implemented in the time-domain. The input voltage waveform is the same as the one for the peak detector model, but due to the long time constants involved, this signal has to be repeated until the output of the detector reaches the steady-state. Finally, the output signal of the QP-detector is applied to the video filter, resulting in an averaging of the signal. **Fig. 5 b)** shows an example of the signals at the input of the detector  $V_{QP,i}$ , at the output  $V_{QP,o}$  and the final signal after the video filter  $V_{VF,o}$ .



**a)**



**b)**

**Fig. 5a)** Quasi-peak detector circuit. **b)** Simulation result.

### III. CONVERTER MODELING

The main source of DM noise is the input current of the PFC-stage. In the boundary conduction mode, the switch is turned on for a constant time  $t_{on}$ , resulting in a peak inductor current proportional to the instantaneous rectified line voltage. During the off-time of the switch, the inductor current decreases and as soon as it reaches zero, the next switching cycle begins. The result is a triangular current waveform with a sinusoidal envelope (**Fig. 6 a)**). Due to the varying turn-off time, the switching frequency is not constant and has a minimum at the peak of the line voltage (**Fig. 6 b)**). The peak current is two times the average current; therefore, the input current spectrum shows high harmonic contents in the range of the switching frequency.

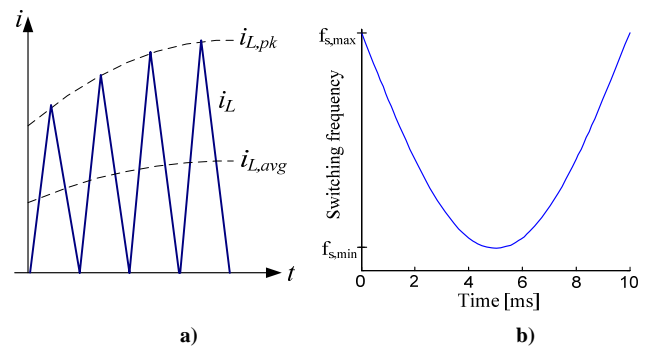


**Fig. 6 a)** Inductor current waveform. **b)** Variation of the switching frequency over a mains half cycle.

The CM noise is caused by the parasitic capacitances from switching nodes to the metal case/ground, which is connected to the protective earth (PE). It is assumed in the following that SMD components are used for the power semiconductors. Consequently, the parasitic capacitances are low compared to transistors mounted on an earthed heat sink. Nevertheless, the CM noise levels exceed the limits and need to be considered in the filter

design. Furthermore, the lamp is typically mounted in an earthed luminaire; therefore, additional capacitances exist between the lamp and the luminaire.

#### A. Calculation of the PFC Waveforms

Due to the variation of the inductor current amplitude and of the switching frequency, a cycle-by-cycle approach is used to calculate the PFC waveforms for one mains half-period [6]. Assuming a constant on-time  $t_{on}$  and DC-bus voltage  $V_{DC}$ , the on-time is given by:

$$t_{on} = \frac{4P_{out}}{V_{AC}^2 \eta} \quad (1)$$

where  $P_{out}$  is the output power of the PFC stage and  $\eta$  the efficiency of the lamp ballast.

Assuming a constant line voltage  $V_{AC}$  during the switching cycle, the current is increasing linearly and the peak current at the end of the on-time is

$$i_{L,pk,n} = \frac{t_{on} \cdot V_{AC} (t_{n-1} + 0.5t_{on})}{L} \quad (2)$$

During the off-time of the switch, the current decreases linearly and the time when  $i_L$  reaches zero is

$$t_{off,n} = \frac{i_{L,pk,n} \cdot L}{V_{DC} - V_{AC} (t_{n-1} + 0.5t_{on})} \quad (3)$$

Equations (3) and (4) are calculated repeatedly for one mains half-period.

The idealized voltage waveform for the CM noise source can be found using:

$$V_{Cp,n} = \begin{cases} 0; & (t_{n-1} < t \leq t_{n-1} + t_{on}) \\ V_{DC}; & (t_{n-1} + t_{on} < t \leq t_n) \end{cases} \quad (4)$$

In case a modulation function is used for noise shaping [7] or improvement of the input current THD, the output of the controller depends on the modulation function. Therefore, equation (1) is not valid and a simulation of the current including the controller is necessary. **Fig. 7** shows the model used for the simulation applied in this paper.

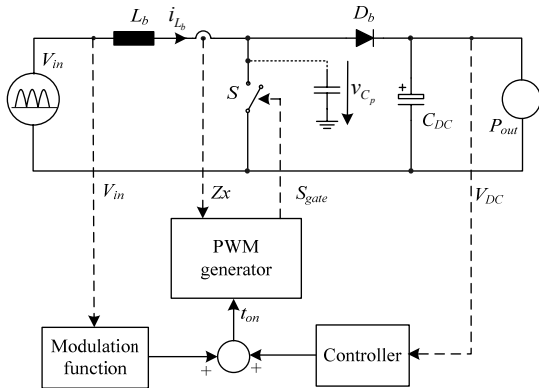


**Fig. 7** Model used for the calculation of the current and voltage waveforms of the PFC.

#### B. Differential Mode Model

**Fig. 8** shows the model used for the calculation of the DM noise spectrum. The LISN is modelled as described in the previous section and the input capacitor of the PFC is modelled with its first order parasitics.

The model is used to derive the transfer function  $G_{DM}(s) = u_{rec}(s)/i_{DM}(s)$  which is required for calculating the voltage spectrum at the input of the test receiver resulting from the inductor current spectrum.

**Fig. 9** shows the comparison of the DM measurement and the simulation result using the propagation model from **Fig. 8**. In band A (9 kHz – 150 kHz) the simulation shows good agreement with the measurement. In band B (150 kHz – 30 MHz) the simulated noise level drops too fast compared to the measurement.

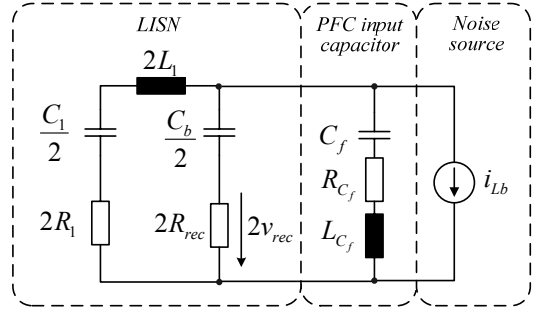


**Fig. 8** DM noise propagation model.

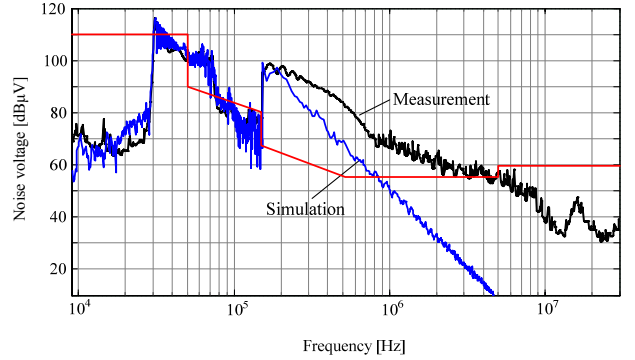


**Fig. 9** Measurement and simulation of the DM peak spectrum.

Comparisons of the simulated results with a circuit simulation using *Simplorer<sup>TM</sup>* showed that the bridge rectifier, which is neglected in the noise propagation model, causes significant deviations and must be included in the calculations of the spectrum.

#### C. Improved Model Including Rectifier

The input current passing through the bridge rectifier  $i_{in}$  is the sum of the inductor current  $i_{Lb}$  and the filter capacitor current  $i_{Cf}$  (cf. **Fig. 10 a**). In **Fig. 10 b** the simulated current  $i_{in}$  using the noise propagation model without rectifier (cf. **Fig. 8**) is shown. The resulting current waveform has also negative values which would be blocked by the rectifier in the real circuit.

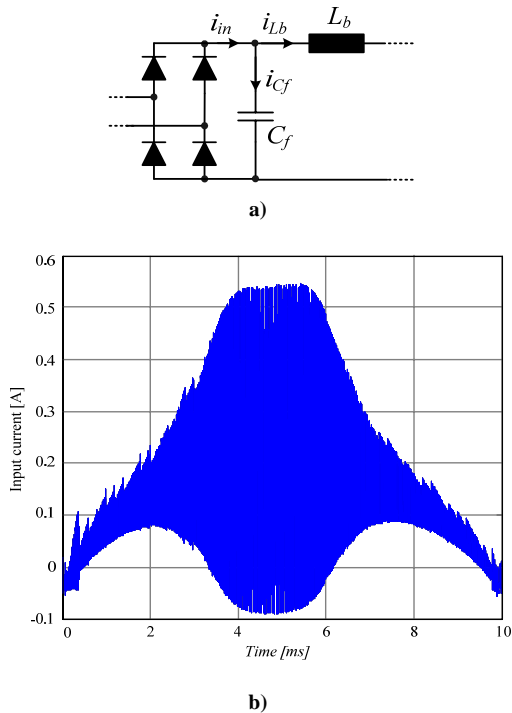


**Fig. 10 a)** Input current without rectifier **b)** Simulation of the input current  $i_{in}$  resulting from the model without rectifier (**Fig. 8**).

This effect of the rectifier is approximated by the following modified simulation procedure:

First, the input current  $i_{in}$  is calculated in the frequency-domain using the noise propagation model without rectifier and then an inverse FFT is used to find the time-domain current waveform (cf. **Fig. 10 b**). The rectifier is then approximated by setting all negative parts of the current to zero. Finally, the noise voltage at the input of the test receiver is calculated using the noise propagation mode shown in (**Fig. 11**). The inclusion of the rectifier in the simulation results in a good agreement of the simulated DM spectrum with measurements (see **Section V**).

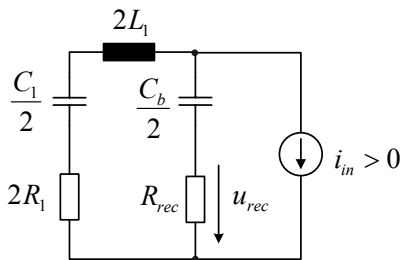


**Fig. 11** Modified noise propagation model.

#### D. Common Mode Model

The main source of CM noise in the PFC is the parasitic capacitance  $C_p$  from the drain node of the PFC switch to the case of the ballast. **Fig. 12 a)** shows the path of the CM noise current  $i_{CM}$  for the case diodes  $D_1$  and  $D_4$  are conducting.

The simplified noise propagation model for the calculation of the CM noise spectrum is shown in **Fig. 12 b)**. Due to the very small parasitic capacitance of

3.4 pF for the considered setup, the DC-blocking capacitors of the LISN and the PFC filter capacitor  $C_f$  can be modeled as short circuits at the frequencies of interest. For the same reason, the inductor  $L_l$  of the LISN and the boost inductor  $L_b$  are assumed to be open.

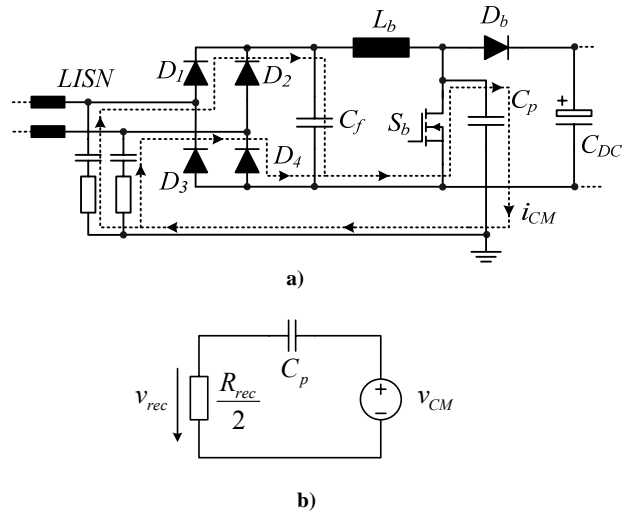


**Fig. 12 a)** CM noise current when  $D_1$  and  $D_4$  conduct. **b)** Simplified CM noise propagation model.

This model is only valid for the case a filter capacitor is used across the input or output terminals of the rectifier. If no capacitor is present, the CM current flows only through the diode  $D_4$  or  $D_3$  because of the high impedance of the boost inductance  $L_b$  [4]. The result is a noise voltage across only one of the LISN impedances, contributing to DM as well as CM noise.

#### IV. IMPLEMENTATION

The simulation method described in the previous sections was implemented in a stand-alone *Java* program (cf. **Fig. 13**). The input parameters for the simulation of the circuit waveforms are the component values and the operating point of the ballast. Additionally, an EMI filter editor allows selecting the type and the values of the filter components which are simulated including first-order parasitics. The simulated filter transfer functions and noise spectrums are either plotted in the program or saved as text files.

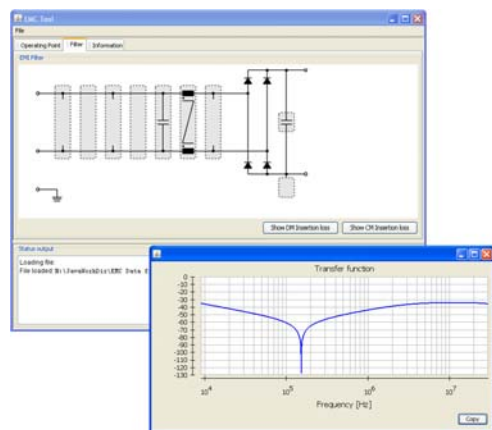


**Fig. 13** Screenshot of the *Java* program showing the filter editor and a calculated filter transfer function.

## V. COMPARISON WITH MEASUREMENTS

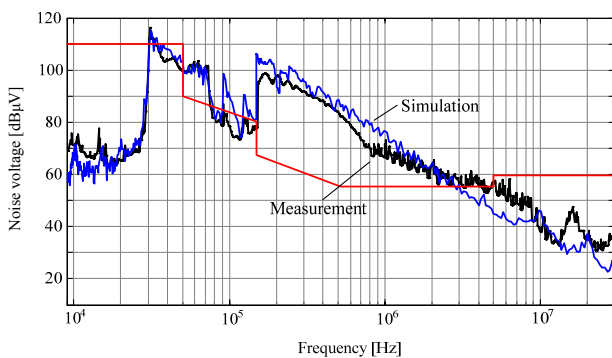
In order to verify the models used for the EMI simulation, EMI measurements have been performed with a 35 W T5 ballast (cf. **Fig. 14**) using a lamp as load. The input filter of the ballast was removed, with the exception of the PFC input capacitor ( $C_f$  in **Fig. 1**). A single phase version of a CM-DM noise separator described in [8] was used to measure the emission modes independently.



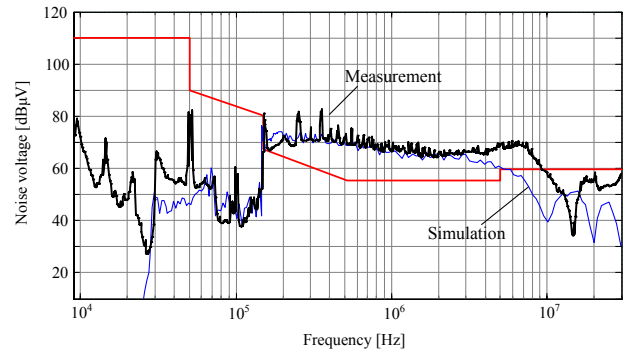
**Fig. 14** Photograph of the 35W ballast and the external DSP control board.

A comparison of the simulated DM spectrum with a DM noise measurement can be seen in **Fig. 15 a)**. The simulation shows good correlation of the simulated results with the measurement over the whole range of the spectrum.

The comparison of the CM simulation with the measurements (cf. **Fig. 15 b)**) shows, that the baseline of the CM spectrum is caused by the parasitic capacitance from the drain of the PFC MOSFET to the case of the ballast. The shape of the CM noise spectrum above 1 MHz depends on the  $dv/dt$  at turn-on/turn-off of the switch, which is only roughly approximated in the presented model. Additionally, the measured spectrum shows peaks at multiples of the inverter switching frequency (50 kHz) which is not yet modeled. The amplitude of the peaks in the range above 150 kHz is important for the design of the CM filter. Therefore, the inverter and the parasitics of the lamp will be modeled in the next step.



**a)**



**b)**

**Fig. 15** Measurement and simulation of **a)** the DM peak spectrum and **b)** the CM peak spectrum.

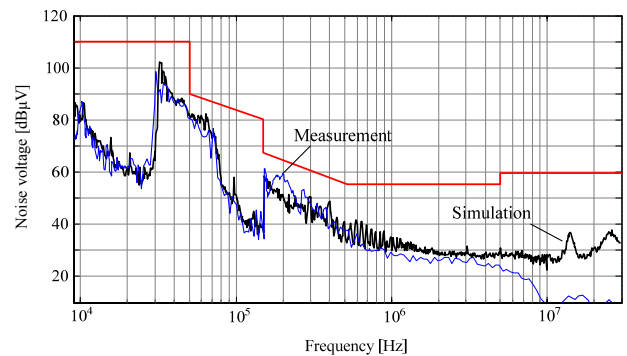


**Fig. 16** Measurement and simulation of the total noise peak spectrum including all EMC filter components.

**Fig. 16** shows the result of a simulation including the filter components  $L_f$  and  $C_p$  (cf. **Fig. 1**), which are modeled in the DM and CM noise propagation models (**Fig. 8** and **Fig. 12 b)**) with their first order parasitics.

## VI. CONCLUSION

In this paper a model for the conducted noise emission of electronics ballasts is derived. There, the significant CM and DM noise sources and paths of the PFC stage have been identified and the influence of the measurement setup has been considered. The model is based on analytical calculations and on simulations, which are all implemented in a stand-alone *Java* program. For validating the model measurement results are presented, which show a very good correspondence between the calculated and the measured spectrum. In a next step, the influence of the CM noise of the inverter stage on the noise spectrum will be derived and implemented in the *Java* program.

## VII. REFERENCES

- [1] M.K. Kazimierczuk, W. Szaraniec, „Electronic ballast for fluorescent lamps”, IEEE Transactions on Power Electronics, Volume 8, Issue 4, Oct. 1993, Page(s): 386 – 395.
- [2] T. Nussbaumer, M.L. Heldwein, J.W. Kolar, “Differential Mode Input Filter Design for a Three-Phase Buck-Type PWM Rectifier Based on Modeling of the EMC Test Receiver”, IEEE Transactions on Industrial Electronics, Volume 53, Issue 5, Oct. 2006, Page(s): 1649 – 1661.

[3] W. Zhang; M.T. Zhang, F.C. Lee, J. Roudet, E. Clavel, "Conducted EMI analysis of a boost PFC circuit", Proceedings of the Twelfth Annual Applied Power Electronics Conference and Exposition, 1997, Volume 1, 23-27 Feb. 1997, Page(s): 223 – 229.

[4] L. Yang; B. Lu; W. Dong; Z. Lu; M. Xu, F.C. Lee, W.G. Odendaal, "Modeling and characterization of a 1 KW CCM PFC converter for conducted EMI prediction", Proceedings of the Nineteenth Annual IEEE Applied Power Electronics Conference and Exposition, 2004, Volume 2, 2004, Page(s): 763 – 769.

[5] J. Meng, W. Ma, L. Zhang, Z. Zhao, "Identification of essential coupling path models for conducted EMI prediction in switching power converters", Proceedings of the IEEE Industry Applications Society 39th Annual Meeting, 2004, Volume: 3, Page(s): 1832- 1839.

[6] D. Kübrich, M. Schmid, T. Dürbaum, "A fast calculation tool for the design of PFC converters-method and application", Proceedings of the 32nd Annual Conference of the IEEE Industrial Electronics Society, 2005, 6-10 Nov. 2005, Page(s): 6 pp.

[7] M. Albach, "An ac-dc converter with low mains current distortion and minimized conducted emissions", Proceedings of the 3rd European Power Electronics Conference, 1989, Vol. 1, p. 457 – 460.

[8] M.L. Heldwein, T. Nussbaumer, F. Beck, J.W. Kolar, "Novel Three-Phase CM/DM Conducted Emissions Separator", Proceedings of the 20th Annual IEEE Applied Power Electronics Conference and Exposition, 2005, Vol. 2, pp. 797 – 802.